fermentation

MDPI

Article

Mixotrophic Syngas Conversion Enables the Production of *meso*-2,3-butanediol with *Clostridium autoethanogenum*

Anne Oppelt, Anton Rückel, Markus Rupp and Dirk Weuster-Botz *

Chair of Biochemical Engineering, School of Engineering and Design, Technical University of Munich, Boltzmannstr. 15, 85748 Garching, Germany; anne.oppelt@tum.de (A.O.); anton.rueckel@tum.de (A.R.); markus.rupp@tum.de (M.R.)

* Correspondence: dirk.weuster-botz@tum.de; Tel.: +49-89-289-15712

Abstract: Providing simultaneously autotrophic and heterotrophic carbon sources is a promising strategy to overcome the limits of autotrophic syngas fermentations. D-xylose and L-arabinose are particularly interesting as they can be obtained by the hydrolysis of lignocellulosic biomass. The individual conversion of varying initial concentrations of these pentoses and D-fructose as reference was studied with *C. autoethanogenum* in fully controlled stirred-tank reactors with a continuous syngas supply. All mixotrophic batch processes showed increased biomass and product formation compared to an autotrophic reference process. Simultaneous CO and D-xylose or L-arabinose conversion was observed in contrast to D-fructose. In the mixotrophic batch processes with L-arabinose or D-xylose, the simultaneous CO and sugar conversion resulted in high final alcohol-to-acid ratios of up to 58 g g^{-1}. L-arabinose was superior as a mixotrophic carbon source because biomass and alcohol concentrations (ethanol and 2,3-butanediol) were highest, and significant amounts of *meso*-2,3-butanediol (>1 g L^{-1}) in addition to D-2,3-butanediol (>2 g L^{-1}) were solely produced with L-arabinose. Furthermore, *C. autoethanogenum* could not produce *meso*-2,3 butanediol under purely heterotrophic conditions. The mixotrophic production of *meso*-2,3-butanediol from L-arabinose and syngas, both available from residual lignocellulosic biomass, is very promising for use as a monomer for bio-based polyurethanes or as an antiseptic agent.

Keywords: *Clostridium autoethanogenum*; syngas fermentation; mixotrophic alcohol production; carbon monoxide conversion; L-arabinose; *meso*-2,3-butandiol

Citation: Oppelt, A.; Rückel, A.; Rupp, M.; Weuster-Botz, D. Mixotrophic Syngas Conversion Enables the Production of *meso*-2,3-butanediol with *Clostridium autoethanogenum*. *Fermentation* **2024**, *10*, 102. https://doi.org/10.3390/fermentation10020102

Academic Editor: Katerina Stamatelatou

Received: 16 January 2024
Revised: 5 February 2024
Accepted: 6 February 2024
Published: 8 February 2024

1. Introduction

In recent years, there has been a significant focus on producing bio-based fuels and chemicals as sustainable alternatives to petrochemicals. Syngas fermentation, a burgeoning field of research, is one of the promising alternatives [1–3]. In syngas fermentation, gas mixtures of CO, H_2, and CO_2 are converted by anaerobic microorganisms into short-chain organic acids and alcohols, which can subsequently be used as bio-based products [4–6]. Biogenic syngas can be produced by gasifying waste biomass, dried green waste, or corn cobs [4,7,8]. Additionally, syngas is obtained from CO-rich waste gas emitted during industrial processes, such as steel production [4,9]. The main components of syngas are CO, CO_2, H_2, and N_2. Thereby, in the gasification process with pure oxygen, N_2 only occurs in the final gas composition if it is used as a dosing medium for the pneumatic conveying of the biomass [10–13]. The advantages of syngas fermentation include its ability to occur in water under mild reaction conditions, such as 30–37 °C and low pressure, as well as the low costs of the self-regenerating biocatalysts [4]. Moreover, these microbes can adapt to a wide range of syngas compositions and exhibit tolerance to various impurities, including sulfur-containing and organic compounds, such as benzene, toluene, or xylene [14–16].

Unicarbonotrophic, acetogenic anaerobes, such as *Clostridium autoethanogenum*, *Clostridium ljungdahlii*, and *Clostridium ragsdalei*, can conserve energy and assimilate carbon through

the reductive acetyl coenzyme A (Acetyl-CoA) pathway, also known as the Wood-Ljungdahl pathway (WLP). The required electrons are derived either from CO or H_2, whereas CO is thermodynamically favored over H_2 [17]. Acetyl-CoA, the key intermediate, is generated through a series of reduction reactions and is then available for anabolism and product formation [18–20]. The acetyl-CoA is formed by consuming adenosine triphosphate (ATP) [1]. This ATP consumption, resulting through the formyl-tetrahydrofolate-synthase, can be offset through either substrate-level phosphorylation, when acetyl-phosphate reacts to acetate by the acetate kinase, or by a membrane-bound ATPase driven by a membrane-bound Rnf complex [1,21].

The aforementioned strictly anaerobic bacteria produce acetate, ethanol, and 2,3-butanediol, whereas *C. carboxidivorans* has the additional ability to produce butyrate, 1-butanol, hexanoate, and 1-hexanol. However, the concentrations of the C4-C6 products remain low, and the production of acids is not particularly favorable [22–24]. *C. autoethanogenum*, being an extensively studied and sequenced acetogen, is already employed for the industrial production of ethanol from steel-mill off-gases [10,25,26].

However, the challenges in syngas fermentation remain the low solubilities of H_2 and CO in water, which may result in gas–liquid mass transfer limitations, the poor alcohol-to-acid ratios and low product concentrations with wild-type strains, and the low biomass densities in submerged syngas fermentation resulting in low volumetric productivities [27]. Therefore, various studies have investigated the optimization of autotrophic cultivation conditions, including partial pressures of the syngas components (nutrient level), pressure, pH, medium composition, and temperature [4,14,28,29]. For instance, *Clostridium aceticum* can utilize CO as a sole source of carbon and energy. However, its ability to withstand higher concentrations of CO is limited [30]. In contrast, *C. autoethanogenum* shows a higher tolerance to increased CO levels [17,28]. Further studies focused on genetically engineered *C. autoethanogenum* and showed enhanced autotrophic growth and product formation [31–36]. Liew et al. [32] discovered that the presence of the CO dehydrogenase isogene acsA is crucial for autotrophic growth while deleting it actually increased product formation. Additionally, novel product routes to value-added molecules, such as 3-hydroxypropionate, 1-propanol, and acetone, have been introduced by applying metabolic engineering [37].

As the aforementioned strategies only lead to limited improvements in the autotrophic formation of products with increased carbon chain lengths (>C2), further strategies are required [4,35,38,39]. For example, co-cultivation of anaerobic microorganisms can form longer-chain alcohols and organic acids, for instance, 1-hexanol and hexanoate, with higher added value through chain elongation [39–43]. In a study by Diender et al. [40], a concentration of hexanoate reaching 1.2 g L^{-1} was achieved through the autotrophic co-culture of *C. autoethanogenum* and the chain elongator *C. kluyveri*. However, the low amount of autotrophic ethanol production remains a limiting factor for chain elongation by *C. kluyveri*. Continuous processes have been studied to enable higher volumetric productivities in syngas fermentations, e.g., continuous stirred-tank bioreactors and cascades thereof, membrane reactors enabling cell retention, as well as biofilm reactors [35,41,44–48]. For instance, Mayer et al. [30] achieved a CO conversion of 70% with *C. aceticum* in a continuously operated stirred-tank bioreactor with a novel submerged microfiltration membrane module that enables total cell retention.

Apart from the WLP, in which anaerob metabolize autotrophic substrates, they can also consume heterotrophic substrates via the Embden–Meyerhof–Parnas (EMP) pathway (glycolysis) [1,21,49,50]. For instance, *Clostridium magnum* grows with a broad spectrum of pentoses, hexoses, glycerol, cellobiose, and maltodextrin, respectively, whereas *C. autoethanogenum* can only use a very limited range of carbohydrates, particularly D-fructose, D-xylose, L-arabinose, and D-ribose, to a lesser extent [25,51]. Hereby, D-xylose and L-arabinose are of particular interest as these pentoses can easily be produced by acid-catalyzed or enzymatic hydrolysis of residual lignocellulosic biomass, such as straw or extracted sugar beet press pulp [52–54].

In two degradation steps, D-fructose is integrated into glycolysis, forming SS-D-fructose-1,6-bisphosphate. However, implementing L-arabinose and D-xylose into the glycolysis is

significantly more complex. In the first step, the sugars are activated to either D-xylose phosphate or L-ribose phosphate. These intermediates are then incorporated into the pentose phosphate pathway (PPP) and degraded to SS-D-fructose-6-phosphate or glyceraldehyde-3-phosphate through several intermediate steps. These metabolites can be assembled into glycolysis and reduced to the central intermediate acetyl-CoA [21,55–57]. Aristilde et al. [57] demonstrated with *Clostridium acetobutylicum* that D-xylose and L-arabinose can also be metabolized via a glycolysis-independent pathway, the phosphoketolase pathway (PKP). However, many questions remain unanswered regarding elucidating metabolic pathways, regulatory mechanisms, and the evaluation of product formation.

Compared to the WLP, glycolysis can generate ATP. However, if, for example, hexose is used as a carbon source for fermentation, two-thirds of the available carbon can be utilized for growth and product formation, whereas the remaining one-third is oxidized to CO_2 during pyruvate decarboxylation [1,49]. However, providing autotrophic and heterotrophic carbon sources simultaneously leads to a biomass yield improvement and is a promising strategy to overcome the limits in autotrophic syngas fermentation. This concept is also known as non-photosynthetic or acetogenic mixotrophy [1,49,50,58]. Previous studies have already shown that several *Clostridia* can metabolize C1 and C5 or C6 molecules simultaneously. Maru et al. [51] studied 17 acetogens to determine their organic and inorganic carbon substrate utilization. Their findings indicate that mixotrophy leads to increased biomass and product yields. The carbon yields of *Thermoanaerobacter kivui* and *Blautia producta* approached nearly 100% carbon fixation in acetate, lactate, and ethanol. Furthermore, *C. ljungdahlii* was genetically modified to ensure that D-glucose was not preferentially but rather simultaneously consumed with syngas. Jones et al. [49] reported the production of acetone using a genetically modified strain of *C. ljungdahlii*, achieving an acetone yield of 92% of the theoretical maximum for mixotrophic conditions with D-fructose. Through C^{13}-labeling of the carbons in the syngas, it was shown that 70% of the acetate was formed from syngas at the maximum. In another study, *C. carboxidivorans* utilized 10 g L^{-1} D-Glucose and a gas mixture with 20% CO, resulting in enhanced alcohol concentrations of up to 9.1 g L^{-1} in the batch process [59].

A study by Mann et al. [60] has already shown that higher CO conversion can be achieved by the simultaneous utilization of D-xylose and gaseous carbon substrates in a fed-batch process with *C. autoethanogenum*. In contrast, Abubackar et al. [61] reported reduced CO utilization of *C. autoethanogenum* in the presence of D-xylose in a STR at pH 5.75. Jones et al. [49] showed simultaneous utilization of 10 g L^{-1} D-fructose and a syngas mixture of ^{13}CO:H_2:$^{13}CO_2$:N_2 (55:20:10:15) in anaerobic flasks with *C. autoethanogenum*. In total, 51–58% of acetate was produced from syngas during the whole batch process, however, ethanol was not measured.

Oliveira et al. [62] compared the ability of *C. autoethanogenum*, *C. ljungdahli*, and *C. ragsdalei* to convert CO-rich syngas in autotrophic batch processes. Among the three strains, *C. autoethanogenum* demonstrated the highest final ethanol and D-2,3-butanediol concentrations and achieved a final alcohol-to-acetate ratio of 7.6 (*w*/*w*). Furthermore, *C. autoethanogenum* is promising with real syngas. Piatek et al. showed an adaptation of this strain by gradually increasing the concentrations of organic components, such as benzene, toluene, and xylenes, during fermentation in anaerobic bottles [16]. The organic components mentioned are typical minor components in the syngas of wood gasification plants [16,63]. As shown before, mixotrophic fermentation processes are promising but sparsely investigated so far with *C. autoethanogenum*. The published results were achieved at uncontrolled reaction conditions in most of the cases, as well as with insufficient and incomplete product analytics with no data on gas consumption or production rates. It remains unclear how the ratio of varying sugar sources to syngas affects the simultaneous carbon utilization and formation of products. Consequently, we first investigate the batch conversion of varying initial concentrations of the two pentoses D-xylose and L-arabinose on growth, product formation, and gas uptake or formation rates with *C. autoethanogenum* under mixotrophic conditions in a fully controlled stirred-tank reac-

tor with continuous gassing. L-arabinose has not been used before under mixotrophic conditions with *C. autoethanogenum*. That is why we opted for an appropriate initial concentration of L-arabinose. Mixotrophic batch processes with the hexose D-fructose are studied as well.

We will show that, in mixotrophic batch processes with *C. autoethanogenum*, the use of varying heterotrophic carbon sources results in higher product concentrations, and either D-xylose or L-arabinose are simultaneously used with CO. Mixotrophic batch processes with L-arabinose performed the best, enabling high final concentrations of biomass and alcohols with low levels of acetate. Most surprisingly, *C. autoethanogenum* is able to produce *meso*-2,3-butanediol in addition to D-2,3-butanediol solely at mixotrophic conditions with L-arabinose as the carbon source.

2. Materials and Methods

2.1. Microorganism, Medium, and Heterotrophic Preculture Preparation

C. autoethanogenum JA1-1 (DSM 10061) was purchased from the German Collection of Microorganisms and Cell Culture (DSMZ, Braunschweig, Germany) as freeze-dried cultures.

The preparation, sterilization, and anaerobization of the media for preculture and reactor cultivation were performed, as reported by Rückel et al. [64]. The composition of the media is listed in the Supporting Information (Table S1).

For the preculture preparations of the reference batch process, 2.5 mL of a stored cryopreserved cell broth of *C. autoethanogenum* with ~0.05 g L^{-1} cell dry weight (CDW) was added to sterile anaerobic 250 mL flasks with 100 mL medium. A total of 5 g L^{-1} D-xylose was used as a heterotrophic carbon source, and 0.4 g L^{-1} cysteine hydrochloride was added as a reducing agent. A total of 5 g L^{-1} of either D-xylose, L-arabinose, or D-fructose was applied for the mixotrophic preculture preparations.

The anaerobic flasks were incubated for 22 h at 37 °C and 100 min^{-1} in an incubator (WIS-20, Witeg, Wertheim, Germany). *C. autoethanogenum* was harvested at the end of the exponential growth phase by centrifugation (10 min, 3620 rcf, Rotica 50 RS, Hettich GmbH & Co. KG, Tuttlingen, Germany) under anaerobic conditions. The separated cells were resuspended with 10 mL anaerobic phosphate-buffered saline (12 mM phosphate) before inoculation of the stirred-tank bioreactor.

2.2. Continuously Gassed Stirred-Tank Bioreactor Setup

All batch cultivations were carried out under continuous gas supply in a fully controlled stainless steel, stirred-tank bioreactor (STR) (KLF2000, Bio-Engineering, Wald, Switzerland). The nominal volume was 2.4 L (d_{tank} = 98 mm) with a working volume of 1 L. The STR was agitated with two six-blade Rushton turbines. A temperature sensor and a heating and cooling rod were used for temperature control. A sterilizable pH sensor (405-DPAS-SC-K8s/120, Mettler Toledo, Giesen, Germany) and a sterilizable redox sensor (Pt4805-DPAS-SC-K8S/120, Mettler Toledo, Germany) were inserted through two side ports of the STR. A total of 3 M NaOH or 0.5 M H_2SO_4 were added via two lid ports for pH control. A pressure probe and a safety valve were installed at the lid as well. A tube was fixed at the baffles inside the STR for the syngas supply via the lid to a sintered frit below the stirrer at the bottom of the reactor. An exhaust gas section guides the reactor off-gas out of the STR. By cooling the off-gas at 2 °C, evaporation is reduced. A sampling valve was installed at the bottom of the STR.

The STR was sterilized in situ at 121 °C for 21 min at 2.2 bar absolute pressure with 1 L medium (without vitamins, L-cysteine hydrochloride, heterotrophic carbon source, and MES). After cooling to 37 °C, 10 mL of vitamin stock solution was added aseptically through a syringe filter with 0.2 µm pore size via a septum (diameter 12 mm, Infors AG, Bottmingen, Switzerland) fixed in a lid inlet. The detailed compositions of the vitamin stock solution are in the Supporting Information (Table S1). The medium was anaerobized for approximately 2 h with 20 NL h^{-1} N_2 and afterward saturated with 5 NL h^{-1} of the syngas mixture for at least 16 h.

Heterotrophic carbon sources were added immediately before inoculation. Therefore, anaerobic, sterile stock solutions were prepared with either 250 g L^{-1} D-xylose, 200 g L^{-1} L-arabinose, or 375 g L^{-1} D-fructose. The volume for achieving initial concentrations of 10 g L^{-1}, 15 g L^{-1}, or 20 g L^{-1} of the varying heterotrophic carbon sources in the STR were added through a septum with single-use syringes (BD Discardit II, Becton Dickinson, Franklin Lakes, NJ, USA) and sterile needles (Sterican 0.9 × 70 mm, B. Braun, Melsungen, Germany). A total of 10 mL of 40 g L^{-1} L-cysteine hydrochloride stock solution was finally added as a reducing agent before inoculation with *C. autoethanogenum* to achieve an initial cell dry weight concentration of 0.03 g L^{-1}.

All batch processes were performed at a constant stirrer speed of 1200 rpm (volumetric power input of 15.1 W L^{-1}). The temperature was controlled at 37 °C, and the pH was kept at pH 6.0. The batch cultivations were carried out at 1 bar absolute pressure. The STR was continuously gassed with 5 NL h^{-1} (0.083 vvm).

An artificial syngas mixture was prepared using a gas mixing system with four thermal mass flow controllers (P-702CV-6K0R-RAD-33-V, Bronkhorst, Reinach, Switzerland). The flow rates of the syngas components were adjusted to 1.95 NL h^{-1} (p_{N2} = 390 mbar; 39.4 (*v*/*v*)) N_2, 1.50 NL h^{-1} (p_{CO} = 300 mbar; 29.8 (*v*/*v*)) CO, 1.10 NL h^{-1} (p_{H2} = 220 mbar; 22.0 (*v*/*v*)) H_2, and 0.45 NL h^{-1} (p_{CO2} = 90 mbar;8.9 (*v*/*v*)) CO_2. The flow rates of the heterotrophic batch process were adjusted to 4.55 NL h^{-1} (p_{N2} = 910 mbar; 90.1 (*v*/*v*)) N_2 and 0.45 NL h^{-1} (p_{CO2} = 90 mbar; 8.9 (*v*/*v*)) CO_2.

2.3. Analytical Methods

During the batch processes, liquid samples for biomass and product concentrations were collected via the sampling valve on the bottom of the STR.

The samples' optical density (OD_{600}) was measured at 600 nm in a UV–Vis spectrophotometer (Genesys 10S UV–Vis, Thermo Scientific, Neuss, Germany). The measurements of OD_{600} were carried out in technical triplicates for each sample. In general, the biomass concentration was estimated based on the optical density with a correlation factor of 0.38 g L^{-1} OD^{-1} [62,64,65].

The product concentrations (organic acids and alcohols) were analyzed with high-performance liquid chromatography (HPLC) (LC-2030C, Shimadzu, Kyoto, Japan). The HPLC analysis was performed using a cation exchange separation column (Aminex HPX-87H, Bio-Rad, Munich, Germany) and a refractive index detector (RID-20A, Shimadzu, Kyoto, Japan). All measurements were carried out under isocratic elution conditions at a constant flow rate of 0.6 mL min^{-1} 5 mM H_2SO_4 and a column oven temperature of 60 °C.

The volumetric exhaust gas flow rate was detected online with a thermal mass flow meter (MFM) (F-101D-RAD-33-V, Bronkhorst, Reinach, Switzerland) with a step time of 30 s. The off-gas composition of the syngas components N_2, CO, CO_2, and H_2 was analyzed with a micro-gas chromatograph (μGC) (micro-GC 450, Agilent Technologies, Waldbronn, Germany). The μGC consists of three independent channels with thermal conductivity detectors and separation columns. With the first channel (molecular sieve, argon as a carrier gas, column temperature 80 °C, initial pressure of 250 kPa), permanent gases like H_2, N_2, and CO can be identified. The second channel (PlotPQ, helium as carrier gas, column temperature 80 °C, initial pressure of 150 kPa) can detect CO_2, NH_3, and NO_x. With channel 3 (CP-Sil 5, helium as carrier gas, column temperature 45 °C, initial pressure 100 kPa), CO_2 and H_2S can be analyzed. Exhaust gas samples were analyzed with a step time of 12 min. The volumetric gas uptake and production rates of CO, CO_2, and H_2 were calculated based on the μGC-measured exhaust gas concentrations and the measured volumetric exhaust gas flow rates.

3. Results and Discussion

3.1. Autotrophic Batch Processes with C. autoethanogenum

Two independent autotrophic batch processes were performed with *C. autoethanogenum* as a reference in the stirred-tank bioreactor with continuous gassing. The selected reference

data are shown in Tables 1 and 2. The chosen artificial syngas composition is based on the publication of Rückel et al. [64]. After a processing time of 145 h, a maximum CDW concentration of 0.49–0.54 g L^{-1} was observed. The highest product concentrations were 1.26–1.50 g L^{-1} acetate, 2.63–2.83 g L^{-1} ethanol, and 0.34 g L^{-1} D-2,3-butanediol, respectively. This is within the estimation error of previously published results, except for the final D-2,3-butanediol concentration (0.52 g L^{-1}) [64]. The maximal CO uptake rate was 7.91–8.15 mmol L^{-1} h^{-1} with a total CO consumption of 626.31–652.06 mmol C L^{-1} in the autotrophic batch processes and a CO:CO_2 ratio of 1.49–1.56, respectively. The carbon balance was closed to 90.66–91.10% (Table 1). Overall, both autotrophic batch processes demonstrated consistent results.

Table 1. Selected process performance data of the autotrophic and mixotrophic batch processes with varying initial D-xylose concentrations ($c_{D\text{-}xylose,initial}$) with *C. autoethanogenum* in stirred-tank bioreactors with continuous gassing (390 mbar N_2, 300 mbar CO, 220 mbar H_2, and 90 mbar CO_2). Minimal and maximal values of two individual autotrophic batch processes are indicated (F_{gas} = 5 NL h^{-1}, 37 °C, pH 6.0, and P V^{-1} = 15.1 W L^{-1}). The final product concentrations are the average of the measured data points between 120–144 h. Excluding the marked concentrations (*).

$c_{D\text{-}xylose,initial}$, g L^{-1}	0 min/max	10.3	13.7	19.3
μ_{max}, h^{-1}	0.06	0.26	0.25	0.25
CDW_{max}, g L^{-1}	0.49–0.54	1.11	1.50	1.65
$c_{Acetate,final}$, g L^{-1}	1.11–1.15	0.10	0.24	0.40
$c_{Ethanol,final}$, g L^{-1}	2.62–2.77	5.31	7.38	8.68
$c_{D\text{-}2,3\text{-}butanediol,final}$, g L^{-1}	0.31–0.32	0.45	0.99 (*)	1.56 (*)
$Ratio_{Alcohol,final:Acetate,final}$, g g^{-1}	2.64–2.68	57.60	34.88	25.60
Carbon in medium, mmol C L^{-1}	9.94	9.94	9.94	9.94
Carbon in biomass, mmol C L^{-1}	15.67–17.10	35.10	47.43	52.24
Carbon in products, mmol C L^{-1}	147.15–160.19	409.32	523.79	620.24
CO consumption, mmol C L^{-1}	626.31–652.06	703.31	864.10	1064.56
CO_2 production, mmol C L^{-1}	400.96–438.80	652.94	611.80	1067.11
CO cons./CO_2 prod., -	1.49–1.56	1.08	1.41	1.00
$CO\ consumption_{max}$, mmol L h^{-1}	7.91–8.15	24.31	28.33	28.56
C-balance (recovery), %	90.66–91.10	105.10	90.01	101.24

Table 2. Selected process performance data of the autotrophic and mixotrophic batch processes with varying initial L-arabinose concentrations ($c_{L\text{-}arabinose,initial}$) with *C. autoethanogenum* in stirred-tank bioreactors with continuous gassing (390 mbar N_2, 300 mbar CO, 220 mbar H_2, and 90 mbar CO_2). Minimal and maximal values of two individual autotrophic batch processes and two mixotrophic processes with 14.2 g L^{-1} and 14.7 g L^{-1} are indicated (F_{gas} = 5 NL h^{-1}, 37 °C, pH 6.0, and P V^{-1} = 15.1 W L^{-1}). The final product concentrations are the average of the measured data points between 120 and 144 h.

$c_{D\text{-}arabinose,initial}$, g L^{-1}	0 min/max	9.8	14.2–14.7 min/max	18.8
μ_{max}, h^{-1}	0.06	0.29	0.20–0.27	0.21
CDW_{max}, g L^{-1}	0.49–0.54	0.82	1.66–1.68	1.80
$c_{Acetate,final}$, g L^{-1}	1.11–1.15	1.19	0.19–0.50	1.18
$c_{Ethanol,final}$, g L^{-1}	2.62–2.77	3.77	8.97–9.18	9.39
$c_{D\text{-}2,3\text{-}butanediol,final}$, g L^{-1}	0.31–0.32	1.25	1.11–2.08	2.07
$c_{meso\text{-}2,3\text{-}butanediol,final}$, g L^{-1}	-	0.10	0.92–1.08	1.07
$Ratio_{Alcohol,final:Acetate,final}$, g g^{-1}	2.64–2.68	4.30	24.68–57.89	10.61
Carbon in medium, mmol C L^{-1}	9.94	9.94	9.94	9.94
Carbon in biomass, mmol C L^{-1}	15.67–17.10	25.80	52.60–53.20	56.84
Carbon in products, mmol C L^{-1}	147.15–160.19	133.86	557.05–611.36	649.18
CO consumption, mmol C L^{-1}	626.31–652.06	388.59	1601.10–1698.14	1538.24
CO_2 production, mmol C L^{-1}	400.96–438.80	505.61	1274.15–1284.48	1298.70
CO cons./CO_2 prod., -	1.49–1.56	0.77	1.26–1.32	1.18
$CO\ consumption_{max}$, mmol L h^{-1}	7.91–8.15	8.57	45.59–45.88	37.01
C-balance (recovery), %	90.66–91.10	91.87	90.51–92.83	92.27

3.2. Mixotrophic Batch Processes with D-Xylose

Figure 1 illustrates the impact of varying initial D-xylose concentrations on the growth, formation of products, and CO consumption of *C. autoethanogenum* in a mixotrophic batch process in a STR with continuous gassing. The initial D-xylose concentrations were varied between 10.3 g L^{-1} (330 mmol C L^{-1}), 13.7 g L^{-1} (440 mmol C L^{-1}), and 19.3 g L^{-1} (644 mmol C L^{-1}). The simultaneous utilization of D-xylose and CO was observed in all reactors (Table S1a,b). The maximum CO uptake rates were measured shortly after D-xylose was entirely consumed. After reaching the maximum CO uptake rates, a rapid decline in CO conversion took place in all mixotroph batch processes. By the end of the batch processes, the CO uptake rates converged to that of the autotrophic reference process. Total CO consumption increased with increasing initial D-xylose concentrations (Table 1). No H_2 uptake was noticed (Supporting Information; Figure S1). As expected, biomass and final product concentrations increased with increasing initial D-xylose concentrations, with the exception of acetate (Figure 1).

Acetate formation was initiated right after the batch processes started (Figure 1d). While both carbon sources were available, a notable rise in acetate formation was observed. A decrease was noticed once the maximum acetate concentration was reached and the initial D-xylose was consumed. At the end of all mixotrophic processes, there was almost no noticeable acetate concentration. However, the higher the initial D-xylose concentrations, the greater the maximal acetate concentrations. In the mixotrophic process utilizing 19.3 g L^{-1} D-xylose, a maximal concentration of 6.42 g L^{-1} acetate was achieved. This represents an increase of 470% compared to the autotrophic reference process. At the process end, the final acetate concentration was 0.40 g L^{-1}, resulting in a decrease of 60% compared to the reference. A similar curve shape can be seen in the CDW concentrations.

Immediately after inoculation, the growth of *C. autoethanogenum* commenced without any *lag* phase in all mixotrophically operated reactors (Figure 1c). After reaching the CDW concentration maximum after the total consumption of D-xylose, a decrease in CDW concentrations could be observed up to 72 h after the process started. At this point, the CDW concentrations remained constant until the processes ended. Here, as before, an increased initial supply of D-xylose led to the attainment of higher maximal CDW concentrations. During the batch process with an initial D-xylose of 19.3 g L^{-1}, the maximal CDW concentration reached 1.65 g L^{-1}, an increase by a factor of three compared to the autotrophic reference process. Almost the same maximal specific growth rates of *C. autoethanogenum* were estimated in all three mixotrophic batch processes in the exponential growth phase (0.26 h^{-1} with 10.3 g L^{-1} D-xylose, 0.25 h^{-1} with 13.7 g L^{-1} or 19.3 g L^{-1} D-xylose). The decrease of CDW concentrations after the complete conversion of D-xylose was already observed in a mixotrophic process in the study of Mann et al. [60]. While the WLP occurs with no ATP net gain, glycolysis provides an abundance of ATP [21]. With the additional available ATP and reduction equivalents from glycolysis, the energy limitation can be overcome in the WLP until the sugar source is depleted.

After approximately 8 h, the ethanol production commenced in all mixotrophic batch processes (Figure 1e). The ethanol concentrations in all reactors increased steadily up to 48 h and then stagnated until the processes ended. All three mixotrophic batch processes showed an improvement in ethanol concentration compared to the autotrophic reference process. The greater the amount of initial D-xylose used, the greater the maximum ethanol concentration achieved. Compared to the autotrophic reference, the mixotrophic process utilizing 19.3 g L^{-1} D-xylose yielded 8.68 g L^{-1} ethanol, a significant enhancement of 220%. However, the ethanol concentration experienced a substantial boost once the acetate concentration began to decrease. Ethanol can also be produced indirectly via acetate and ferredoxin-dependent aldehyde:ferredoxin oxidoreductase by *C. autoethanogenum* [66]. Even before the conversion of acetate to ethanol, a significantly reduced redox potential (Supporting Information; Figure S3) was measured in all three batch processes. This could be due to an excess of reduced ferredoxins, which the oxidoreductase requires to convert acetate to acetaldehyde. Ferredoxin can exhibit a redox potential of up to −500 mV [21].

It can be provided either by the Rnf complex or by the bifurcation of hydrogenase, in which case no hydrogen uptake is observed (Supporting Information; Figure S1) [21]. Once the ethanol concentration remained constant, the redox potential stagnated and increased toward the process's end. This may be due to the decreased ratio of reduced and oxidized ferredoxin.

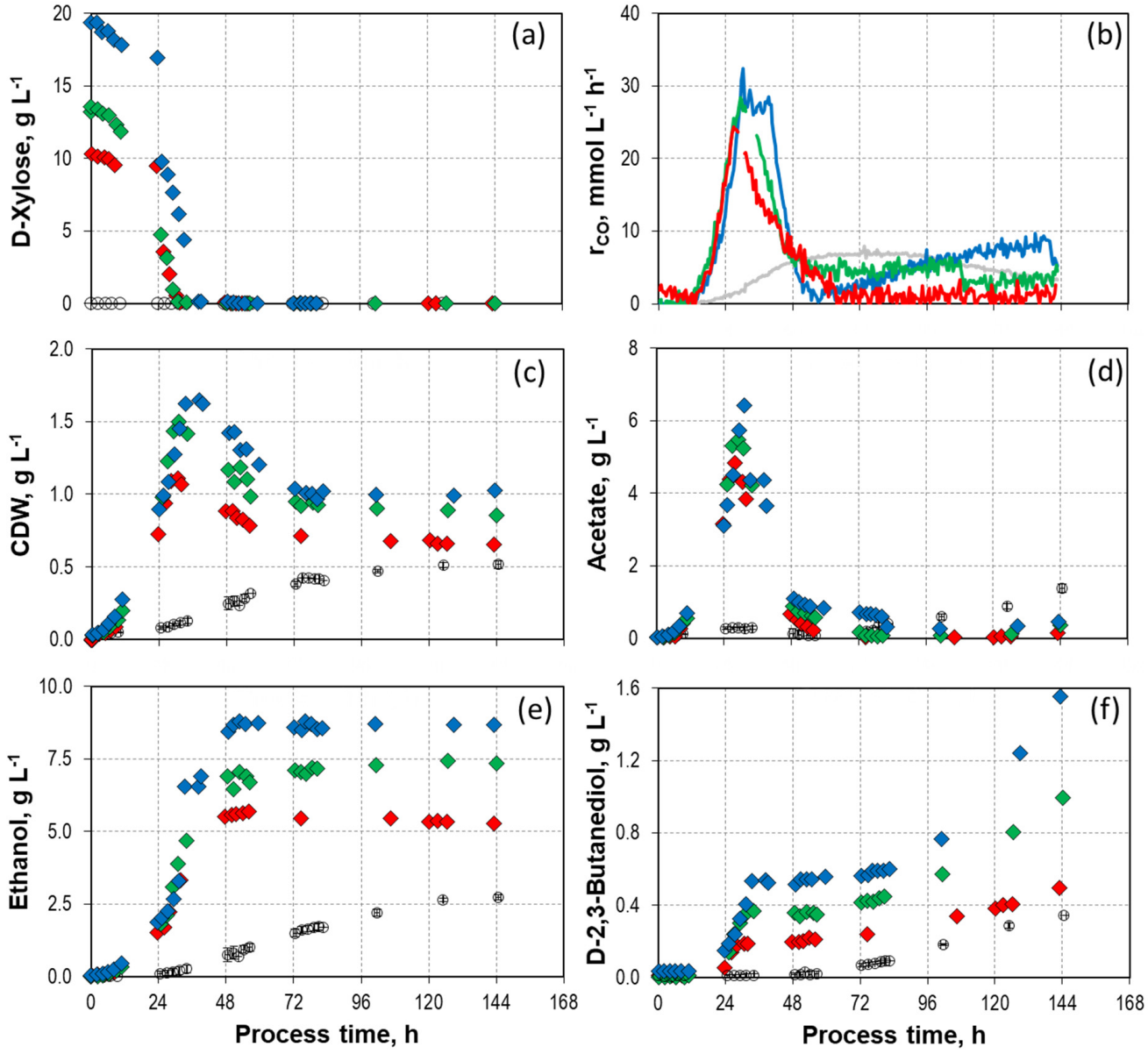

Figure 1. Process performance of mixotrophic batch processes with varying initial D-xylose concentrations (◆ 10.3 g L^{-1}, ◆ 13.7 g L^{-1}, ◆ and 19.3 g L^{-1}) with *C. autoethanogenum* in stirred-tank bioreactors with continuous gassing (390 mbar N_2, 300 mbar CO, 220 mbar H_2, and 90 mbar CO_2) compared to the autotrophic reference batch process (open symbols). (F_{gas} = 5 NL h^{-1}, 37 °C, pH 6.0, and P V^{-1} = 15.1 W L^{-1}). (**a**) D-xylose concentration; (**b**) Carbon monoxide uptake rate; (**c**) Cell dry weight concentration (CDW); (**d**) Acetate concentration; (**e**) Ethanol concentration; (**f**) D-2-3-butandediol concentration. The error bars indicate the minimum and maximum values of two individual autotrophic batch processes.

The D-2,3-butanediol formation was decoupled from growth (Figure 1f). In all mixotrophic processes, the D-2,3-butanediol concentration steadily increased until the heterotrophic carbon source was consumed, and the highest level of CO uptake was

achieved. Subsequently, the D-2,3-butanediol concentration remained constant, like ethanol and acetate, until a processing time of 72 h. However, after that point, there was a renewed increase in formation across all mixotrophic processes until the processes ended. While this phenomenon was also observed in the autotrophic reference process, it was more prominent in the mixotrophic processes. The highest D-2,3-butanediol concentration of 1.56 g L^{-1} was achieved at the mixotrophic process with the highest initial D-xylose concentration. This represents a significant improvement of 280% compared to the autotrophic reference process. The formation of D-2,3-butanediol is suggested to be a result of an excess of available reduction equivalents [15,67].

All mixotrophic processes' carbon balances varied between 90% and 105% recovery. The strong improvement in alcohol production was also reflected in the final alcohol-to-acid ratios. What is particularly significant is that once the maximal CDW concentration was achieved, acetate was completely converted to ethanol regardless of the initial D-xylose concentrations. The final alcohol-to-acid ratio of the process with 10.3 g L^{-1} D-xylose was 57.60 g g^{-1}, and the batch processes with 13.7 g L^{-1} D-xylose and 19.3 g L^{-1} D-xylose showed alcohol-to-acid ratios of 34.88 g g^{-1} and 25.60 g g^{-1}, respectively, in contrast to the alcohol-to-acid ratio of the autotrophic reference process (2.64–2.68 g g^{-1}). The results of Mann et al. [60], where a simultaneous utilization of D-xylose and CO was studied with *C. autoethanogenum* in a fed-batch process, showed no conversion of acetate to ethanol. As a result, the final concentration of acetate exceeded 18.28 g L^{-1}, while the final concentration of ethanol was 1.77 g L^{-1} (final alcohol-to-acetate ratio of ~0.1 g g^{-1}). The difference to our study may be that D-xylose is strongly limiting in the fed-batch process.

Due to the observed simultaneous consumption of the heterotrophic and autotrophic carbon sources, *C. autoethanogenum* shows the ability to effectively use both metabolic pathways in parallel. The impact of heterotrophic carbon sources on carbon fixation via the WLP was previously studied with other *Clostridia* [1,56]. Thereby, carbon catabolite repression (CCR) presents an adverse scenario, which was not observed in our study with *C. autoethanogenum*. Abubacker et al. [61] similarly observed CCR with *C. autoethanogenum* during mixotrophic D-xylose conversion with 100% CO in a batch process in a STR at pH 5.75. Their findings revealed that D-xylose and CO cannot be metabolized simultaneously. Only after the total consumption of D-xylose, CO was consumed, but, compared to a purely autotrophic process, the CO consumption was still reduced. The contrasting outcome to our study may be due to differences in the gas mixture, composition of the liquid cultivation medium, yeast extract concentration (0.5 g L^{-1}), cultivation temperature (30 °C), and pH (5.75) [61].

3.3. Mixotrophic Batch Processes with L-Arabinose

Besides D-xylose, *C. autoethanogenum* is able to metabolize other sugars, such as L-arabinose [25,51]. Figure 2 illustrates the impact of varying initial L-arabinose concentrations on the growth, formation of products, and CO consumption of *C. autoethanogenum* in mixotrophic batch processes in a STR with continuous gassing (Table 2). The initial L-arabinose concentrations varied between 9.8 g L^{-1} (326 mmol C L^{-1}), 14.2–14.7 g L^{-1} (474–489 mmol C L^{-1}), and 18.8 g L^{-1} (624 mmol C L^{-1}).

Similar to the batch processes with D-xylose, the simultaneous utilization of CO and the pentose was also observed in the processes with L-arabinose after inoculation, but it took longer for the sugar source to be consumed entirely compared to D-xylose (Figure 2a,b). In the batch processes with 14.2–14.7 g L^{-1} and 18.8 g L^{-1} L-arabinose, the maximal CO uptake rate was observed when L-arabinose was completely utilized. This had already been observed in the processes with D-xylose. The heterotrophic carbon source was metabolized most rapidly with 14.2–14.7 g L^{-1} L-arabinose, and the CO conversion rate of these batch processes was at the maximum (45.59–45.88 mmol L h^{-1}), which was about 1.5 times and 5 times higher compared to the corresponding process with D-xylose and the autotrophic reference process, respectively. In all mixotrophic batch processes, no H_2 uptake was observed (Supporting Information; Figure S2).

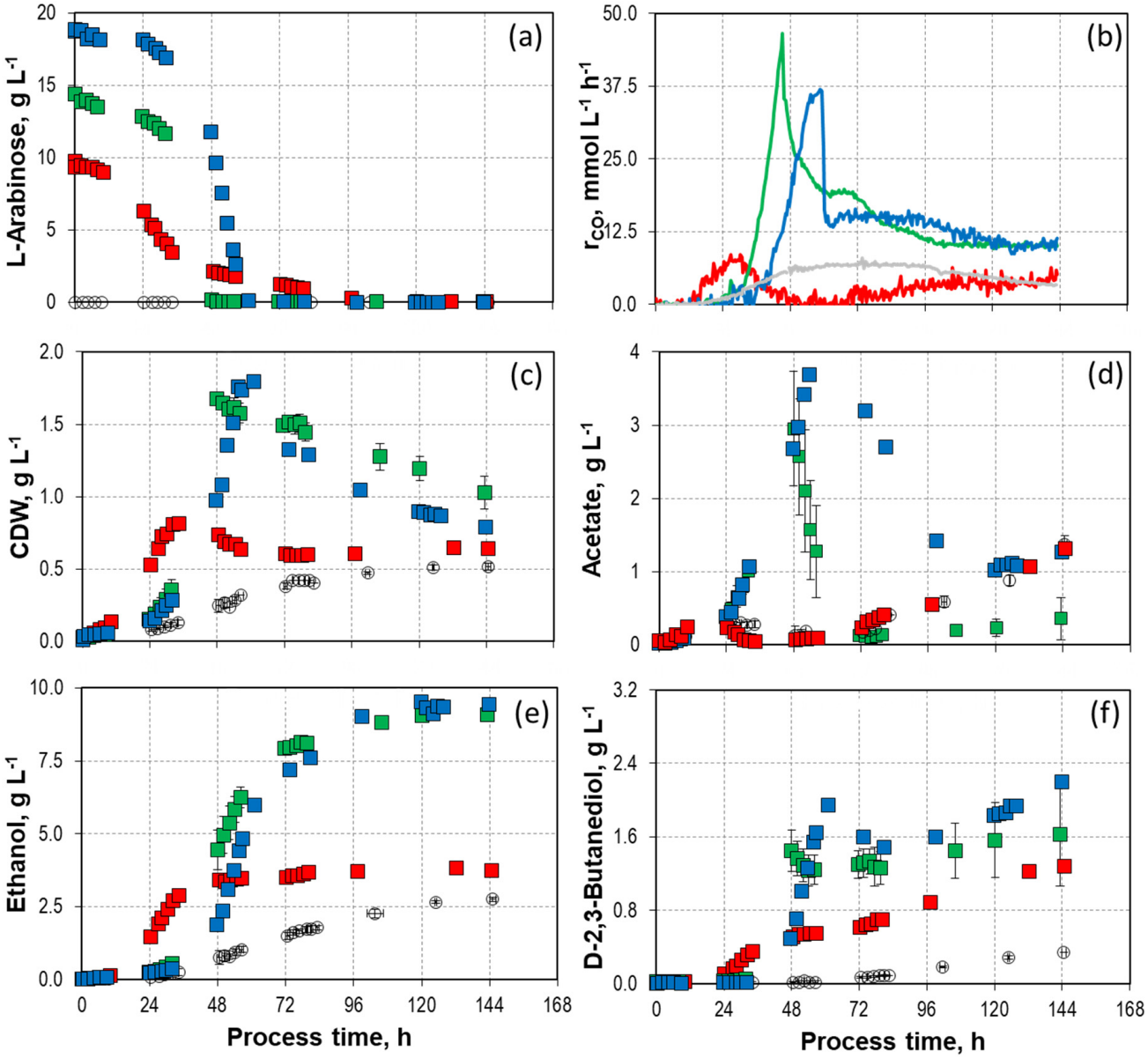

Figure 2. Process performance of mixotrophic batch processes with varying initial L-arabinose concentrations (■ 9.8 g L^{-1}, ■ 14.2/14.7 g L^{-1}, and ■ 18.8 g L^{-1}) with *C. autoethanogenum* in stirred-tank bioreactors with continuous gassing (390 mbar N_2, 300 mbar CO, 220 mbar H_2, and 90 mbar CO_2) compared to the autotrophic reference batch process (open symbols). (F_{gas} = 5 NL h^{-1}, 37 °C, pH 6.0, and P V^{-1} = 15.1 W L^{-1}). (**a**) D-arabinose concentration; (**b**) Carbon monoxide uptake rate; (**c**) Cell dry weight concentration (CDW); (**d**) Acetate concentration; (**e**) Ethanol concentration; (**f**) D-2-3-butandediol concentration. The error bars indicate the minimum and maximum values of two individual autotrophic batch processes and two individual mixotrophic processes with 14.2 g L^{-1}–14.7 g L^{-1} (due to the slight discrepancy between the minimum and maximum values at some data points, not all deviations are visible).

At the two higher initial L-arabinose concentrations a similar trend can be observed in the formation of acetate and CDW as in the mixotrophic batch processes with D-xylose (Figure 2c,d). The concentrations initially rose until complete L-arabinose utilization and then began to decline. The noticeable concentration disparities in acetate degradation between the two independent batch processes with 14.2–14.7 g L^{-1} L-arabinose might be caused by slight temporal variations in full L-arabinose utilization. The acetate degradation rate was reduced in the batch process with the highest initial L-arabinose concentration.

Compared to the mixotrophic batch processes with D-xylose, the decline of the CDW concentration was less rapid when consuming L-arabinose at the two higher initial concentrations and was not constant until the end of the process. This discrepancy explains the higher gas uptake rates observed at the end of the L-arabinose processes compared to the processes with D-xylose.

The batch processes with 14.2–14.7 g L^{-1} and 18.8 g L^{-1} L-arabinose achieved almost identical final ethanol concentrations (9.01–9.18 g L^{-1}, and 9.52 g L^{-1}, respectively) (Figure 2e). In contrast, increasing ethanol concentrations were observed with increasing sugar source utilization in the mixotrophic batch processes with D-xylose. Furthermore, with L-arabinose, there was no significant increase in ethanol formation during acetate degradation. Although the processes with D-xylose showed a higher maximum acetate concentration, both processes with L-arabinose resulted in higher final ethanol concentrations.

The D-2,3-butanediol concentrations rose with higher initial L-arabinose, similar to the observations made with D-xylose (Figure 2f). While the D-2,3-butanediol concentration in the mixotrophic batch processes with D-xylose increased more rapidly toward the end of the process, the final concentrations were higher in the processes with L-arabinose. The mixotrophic batch process utilizing 18.8 g L^{-1} L-arabinose achieved a final concentration of 2.20 g L^{-1} D-2,3-butanediol, 40% higher than the corresponding process with D-xylose.

The process performance of the mixotrophic batch process with 9.8 g L^{-1} L-arabinose was different in almost all performance indicators except D-2,3-butanediol concentrations. Indeed, simultaneous metabolization of CO and L-arabinose was observed as well. However, the conversion of L-arabinose took much longer, and the maximum CO uptake rate was significantly lower compared to the two other mixotrophic batch processes, resulting in lower concentrations of CDW and ethanol. Acetate formation was very much reduced within the first 72 h and shows high similarity compared to the autotrophic reference process. The mixotrophic batch process utilizing 18.8 g L^{-1} L-arabinose achieved a final concentration of 2.20 g L^{-1} D-2,3-butanediol, 40% higher than the corresponding process with D-xylose (Figure 2d). In addition, the maximum CO uptake rate does not coincide with the complete utilization of L-arabinose, as it was observed with the higher initial L-arabinose concentrations.

Interestingly, in all mixotrophic batch processes with L-arabinose, *meso*-2,3-butanediol was produced in addition to D-2,3-butanediol (Figure 3). The highest final *meso*-2,3-butanediol concentrations were measured in the mixotrophic batch processes with the higher initial L-arabinose concentrations (0.92–1.08 g L^{-1} and 1.07 g L^{-1}, respectively). No *meso*-2,3-butanediol production was observed in the autotrophic reference process. In total, a final concentration of 3.14 g L^{-1} 2,3-butanediol was achieved in the mixotrophic batch process with a ratio of 66 to 34 of D-2,3-butanediol to *meso* 2,3-butanediol. So far, the production of only very small concentrations of *meso*-2,3-butanediol was reported with *C. autoethanogenum* (0.2 g L^{-1} 2,3-butanediol with a ratio of 94 to 6 of D-2,3-butanediol to *meso*-2,3-butanediol) [68]. The intracellular metabolite (R)-acetoin is highly prone to spontaneous racemization via an enolate intermediate. Consequently, there is a high probability that a small fraction of the formed (R)-acetoin spontaneously racemizes to (S)-acetoin, which is further reduced to *meso*-2,3-butanediol [66]. The *meso*-2,3-butanediol has a favored orientation of the methyl side chains for producing thermoplastic polyurethanes and is the sole stereoisomer with antibacterial and antiseptic properties [67,69].

3.4. Comparison of Mixotrophic Batch Processes with D-Xylose, L-Arabinose, and D-Fructose

Using 14.2–14.7 g L^{-1} L-arabinose in the mixotrophic batch processes showed high final ethanol and 2,3-butanediol concentrations but also extensive conversion of acetate, thus, an improved final ratio of alcohols to acetate of 24.68–57.89 g g^{-1}. As *C. autoethanogenum* has the ability to metabolize D-fructose [25], a mixotrophic batch process with 16.4 g L^{-1} D-fructose has been performed as well. The process performance is compared to the batch process using 14.2–14.7 g L^{-1} L-arabinose in Figure 4.

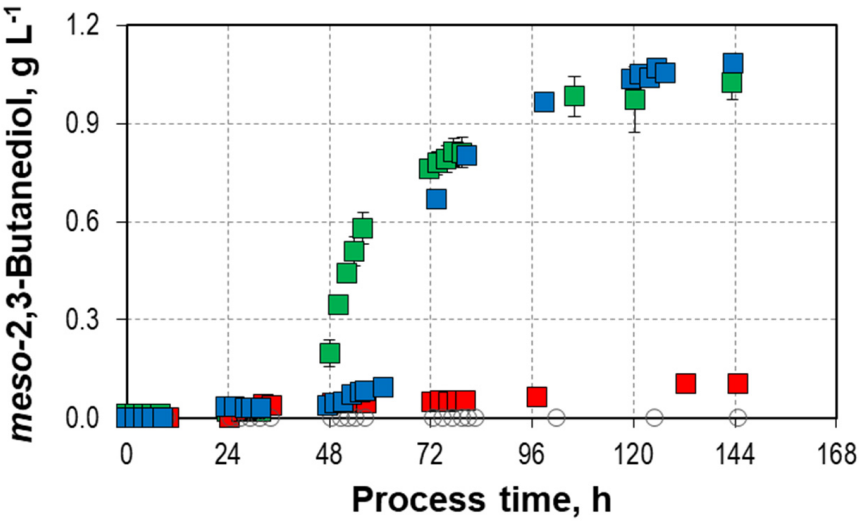

Figure 3. *meso*-2,3-butandiol formation in mixotrophic batch processes with varying initial L-arabinose concentrations (■ 9.8 g L^{-1}, ■ 14.2/14.7 g L^{-1}, and ■ 18.8 g L^{-1}) with *C. autoethanogenum* in stirred-tank bioreactors with continuous gassing (390 mbar N_2, 300 mbar CO, 220 mbar H_2, and 90 mbar CO_2) compared to the autotrophic reference batch process (open symbols). (F_{gas} = 5 NL h^{-1}, 37 °C, pH 6.0, and P V^{-1} = 15.1 W L^{-1}). The error bars indicate the minimum and maximum values of two individual mixotrophic processes with 14.2 g L^{-1} and 14.7 g L^{-1} (due to the slight discrepancy between the minimum and maximum values at some data points, not all deviations are visible).

Unlike in the mixotrophic batch processes involving D-xylose and L-arabinose, there was no simultaneous consumption of CO and D-fructose (Figure 4a,b). During the first 34 h, only D-fructose was utilized by *C. autoethanogenum*, and after a delay of 88 h, CO consumption started. The total CO consumption was 70% lower compared to the autotrophic batch process with L-arabinose. Unlike in the batch process with L-arabinose, complete conversion of acetate to ethanol was not observed. The maximum CDW concentration was much lower compared to the mixotrophic L-arabinose conversion process (Figure 4c,d). The final ethanol concentration was 4.44 g L^{-1}, 50% lower compared to the process using L-arabinose (Figure 4e). Furthermore, only low concentrations of D-2,3-butanediol (0.12 g L^{-1}) were detected (Figure 4f).

These results are in contrast to literature data: Jones et al. [49] demonstrated in anaerobic serum bottles (50 mL medium and 110 mL gaseous headspace) the simultaneous utilization of 10 g L^{-1} D-fructose with a syngas mixture (55% ^{13}CO, 10% $^{13}CO_2$, 20% H_2, 15% N_2) by *C. autoethanogenum*. Approximately 51–58% of acetate was generated from the syngas; the formation of alcohols was not assessed. The differences in process performance might be caused by varying reaction conditions, low power input, and uncontrolled pH drops in the anaerobic flasks.

Summing up, significant variations in carbon assimilation were observed in mixotrophic batch processes with *C. autoethanogenum* compared to the autotrophic reference process. Figure 5 shows the relative final product concentrations, the maximal biomass concentrations, and the maximum specific growth rates of *C. autoethanogenum* in the mixotrophic batch processes with either D-xylose, L-arabinose, or D-fructose with approximately 15 g L^{-1} initial sugar concentration.

In general, due to the increased carbon supply by heterotrophic substrates, clear increases in CDW and product formation are evident, in contrast to the autotrophic batch process. Distinct differences between the various mixotrophic batch processes are obvious: no simultaneous CO and D-fructose conversion was observed with *C. autoethanogenum* compared to the other carbon sources. This led to a carbon flow that mainly contributed to anabolism and acetate formation. The final ratio of alcohol to acetate was significantly lower compared to the processes involving the pentoses. In the mixotrophic batch processes

with L-arabinose and D-xylose, the simultaneous CO and sugar conversion indicates the parallel activity of the WLP and glycolysis.

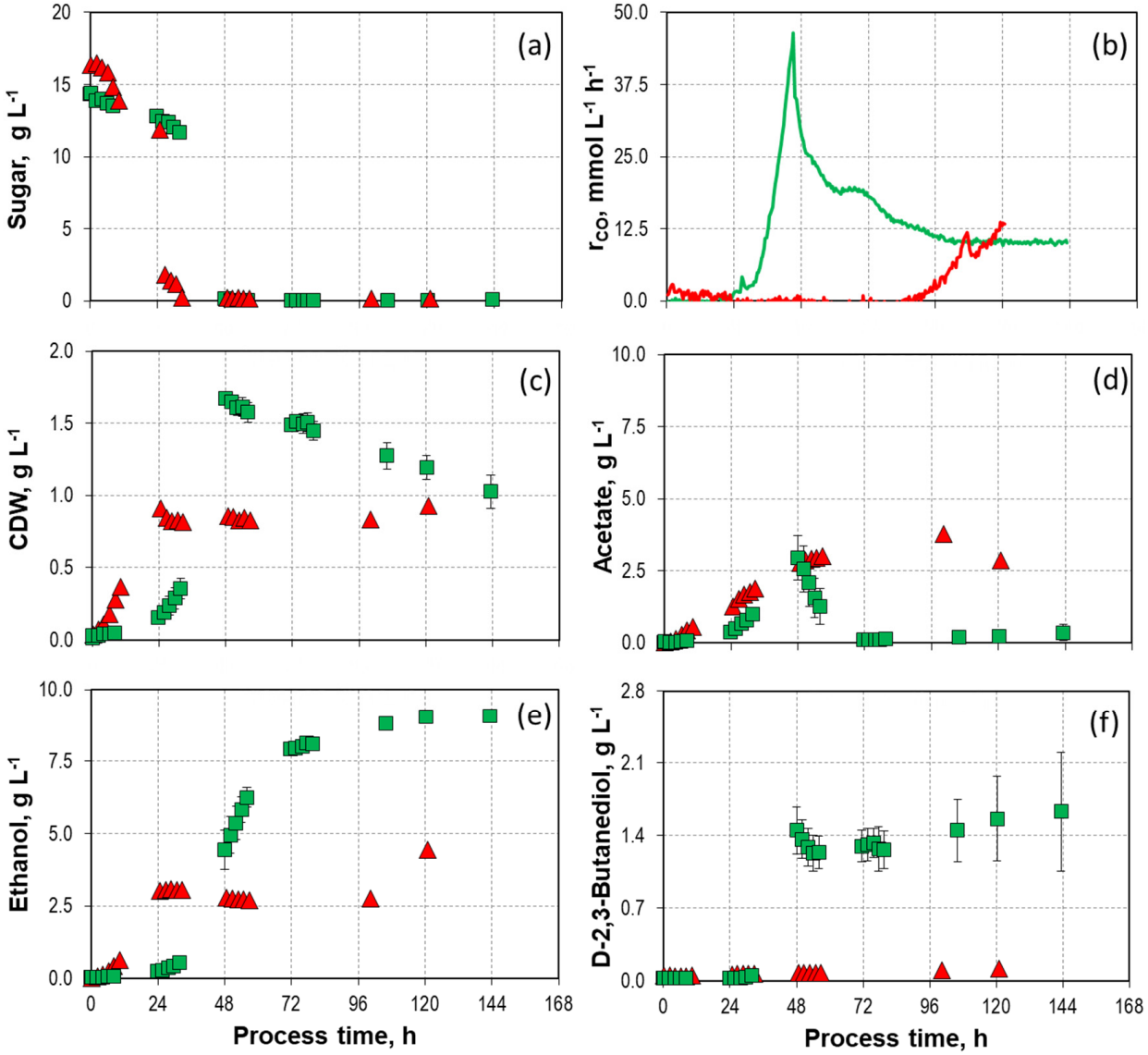

Figure 4. Process performance of mixotrophic batch processes with 16.4 g L^{-1} D-fructose (▲) and 14.2–14.7 g L^{-1} L-arabinose (■) with *C. autoethanogenum* in stirred-tank bioreactors with continuous gassing (390 mbar N_2, 300 mbar CO, 220 mbar H_2, and 90 mbar CO_2). (F_{gas} = 5 NL h^{-1}, 37 °C, pH 6.0, and P V^{-1} = 15.1 W L^{-1}). (**a**) Sugar concentration; (**b**) Carbon monoxide uptake rate; (**c**) Cell dry weight concentration (CDW); (**d**) Acetate concentration; (**e**) Ethanol concentration; (**f**) D-2-3-butandediol concentration. The error bars indicate the minimum and maximum values of two individual mixotrophic processes with 14.2 g L^{-1}–14.7 g L^{-1} (due to the slight discrepancy between the minimum and maximum values at some data points, not all deviations are visible).

Thus, the accumulation of acetate as a by-product was very much reduced, achieving high final alcohol-to-acid ratios. The mixotrophic batch process with 14.2–14.7 g L^{-1} L-arabinose excelled in almost all process performance indicators. CDW and alcohol concentrations were highest, and *meso*-2,3-butanediol was solely produced with L-arabinose.

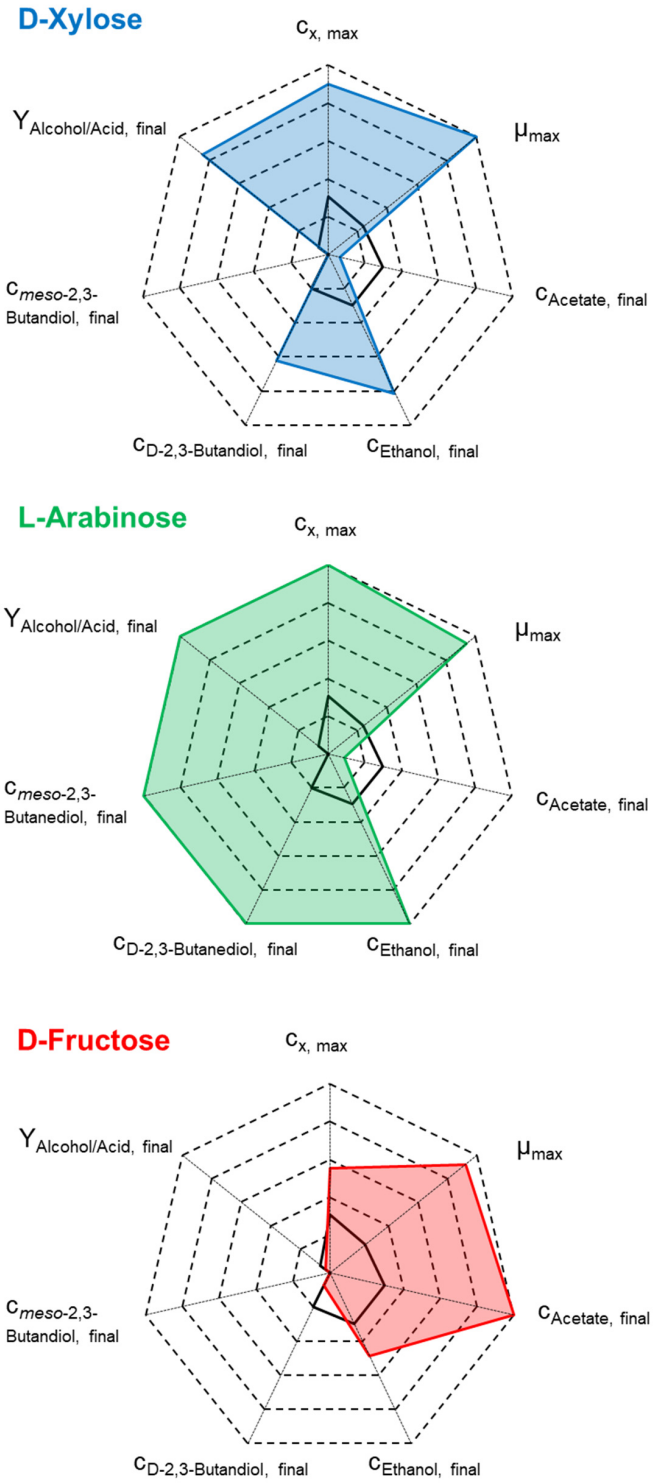

Figure 5. Comparison of $c_{x,max}$, μ_{max}, $c_{p,final}$, and alcohol-to-acid ratio for the performed mixotrophic batch processes with 16.4 g L^{-1} D-fructose (●), 14.2–14.7 g L^{-1} L-arabinose (●), and 13.7 g L^{-1} D-xylose (●) with *C. autoethanogenum* in stirred-tank bioreactors with continuous gassing (390 mbar N_2, 300 mbar CO, 220 mbar H_2, and 90 mbar CO_2) compared to the autotrophic reference batch process (black line). (F_{gas} = 5 NL h^{-1}, 37 °C, pH 6.0, and P V^{-1} = 15.1 W L^{-1}).

Comparing the purely heterotrophic L-arabinose conversion of *C. autoethanogenum* with the mixotrophic batch process (Supporting Information; Figure S4 and Table S2), acetate is predominantly produced instead of alcohol. The acetate concentration reached

a maximum of 8.39 g L^{-1} with no reduction to ethanol as in the mixotrophic process. Consequently, lower quantities of ethanol were obtained, with the highest concentration reaching 1.47 g L^{-1}. After reaching this maximum, the ethanol concentration decreases in parallel to the decrease in biomass concentration. Very small final D-2,3-butanediol concentrations were measured (0.13 g L^{-1}), but the formation of the *meso* stereoisomer was not observed. This clearly shows that *C. autoethanogenum* produces *meso*-2,3-butanediol solely under mixotrophic process conditions with L-arabinose. CO conversion via the WLP pathway provides the required reducing equivalents for the production of the alcohols in the mixotrophic batch process.

4. Conclusions

In mixotrophic batch processes with *C. autoethanogenum*, there were notable differences in carbon assimilation compared to the autotrophic process. The additional use of heterotrophic substrates resulted in higher product concentrations. The various carbon sources (D-xylose, L-arabinose, and D-fructose) displayed distinct variations in CO and sugar conversion. Whereas with D-fructose no simultaneous conversion of CO was observed, *C. autoethanogenum* can utilize CO and either D-xylose or L-arabinose in parallel. The mixotrophic batch processes utilizing L-arabinose performed best, exhibiting the highest concentrations of biomass and alcohols, and low levels of final acetate. When comparing the purely heterotrophic conversion of L-arabinose to a mixotrophic process, acetate was primarily produced instead of the preferred alcohols. Under mixotrophic conditions with L-arabinose, *C. autoethanogenum* exclusively produced *meso*-2,3-butanediol.

Supplementary Materials: The following supporting information can be downloaded at: https://www.mdpi.com/article/10.3390/fermentation10020102/s1, Table S1: Composition of the liquid cultivation medium [65]) used for precultures in anaerobic shaken bottles and batch processes in stirred-tank bioreactors; Table S2: Selected process performance data of the mixotrophic batch processes with 16.4 g L^{-1} D-fructose and the heterotrophic batch process with 14.4 g L^{-1} L-arabinose with *C. autoethanogenum* in stirred-tank bioreactors with continuous gassing; Figure S1: (a) CO_2 formation rate and (b) H_2 uptake rate of mixotrophic batch processes with varying initial D-xylose concentrations (10.3 g L^{-1}, 13.7 g L^{-1}, and 19.3 g L^{-1}) with *C. autoethanogenum* in stirred-tank bioreactors with continuous gassing compared to the autotrophic reference batch process; Figure S2: (a) CO_2 formation rate and (b) H_2 uptake rate with varying initial L-arabinose concentrations (9.8 g L^{-1}, 14.2/14.7 g L^{-1}, and 18.8 g L^{-1}) with *C. autoethanogenum* in stirred-tank bioreactors with continuous gassing compared to the autotrophic reference batch process; Figure S3: Redox-potential of mixotrophic batch processes (a) with varying initial D-xylose concentrations (10.3 g L^{-1}, 13.7 g L^{-1}, and 19.3 g L^{-1}) and (b) with varying initial L-arabinose concentrations (9.8 g L^{-1}, 14.2/14.7 g L^{-1}, and 18.8 g L^{-1}) with *C. autoethanogenum* in stirred-tank bioreactors with continuous gassing compared to the autotrophic reference batch process; Figure S4: Process performance of a heterotrophic batch process with 14.4 g L^{-1} L-arabinose compared to a mixotrophic batch process with 14.2/14.7 g L^{-1} L-arabinose with *C. autoethanogenum* in stirred-tank bioreactors with continuous gassing.

Author Contributions: Conceptualization, A.O. and D.W.-B.; methodology, A.O.; investigation, A.O., A.R. and M.R.; discussion and analysis, A.O., A.R., M.R. and D.W.-B.; writing—original draft preparation and visualization, A.O.; writing—review and editing, D.W.-B.; supervision, project administration, funding acquisition, D.W.-B. All authors have read and agreed to the published version of the manuscript.

Funding: This research was funded by the European Union's Horizon 2020 Research and Innovation Program under Grant Agreement N°. 101006873 (GOLD).

Institutional Review Board Statement: Not applicable.

Informed Consent Statement: Not applicable.

Data Availability Statement: The original contributions presented in the study are included in the article/Supplementary Material; further inquiries can be directed to the corresponding author/s.

Acknowledgments: The support of Anne Oppelt by the TUM Graduate School is acknowledged.

Conflicts of Interest: The authors declare no conflicts of interest.

References

1. Fast, A.G.; Schmidt, E.D.; Jones, S.W.; Tracy, B.P. Acetogenic mixotrophy: Novel options for yield improvement in biofuels and biochemicals production. *Curr. Opin. Biotechnol.* **2015**, *33*, 60–72. [CrossRef] [PubMed]
2. Bessou, C.; Ferchaud, F.; Gabrielle, B.; Mary, B. Biofuels, greenhouse gases and climate change. *Agron. Sustain. Dev.* **2011**, *31*, 1–79. [CrossRef]
3. Asimakopoulos, K.; Gavala, H.N.; Skiadas, I.V. Reactor systems for syngas fermentation processes: A review. *Chem. Eng. J.* **2018**, *348*, 732–744. [CrossRef]
4. Abubackar, H.N.; Veiga, M.C.; Kennes, C. Biological conversion of carbon monoxide: Rich syngas or waste gases to bioethanol. *Biofuel. Bioprod. Bioref.* **2011**, *5*, 93–114. [CrossRef]
5. Griffin, D.W.; Schultz, M.A. Fuel and chemical products from biomass syngas: A comparison of gas fermentation to thermochemical conversion routes. *Env. Prog. Sustain. Energy* **2012**, *31*, 219–224. [CrossRef]
6. Munasinghe, P.C.; Khanal, S.K. Biomass-derived syngas fermentation into biofuels: Opportunities and challenges. *Bioresour. Technol.* **2010**, *101*, 5013–5022. [CrossRef]
7. Kremling, M.; Briesemeister, L.; Gaderer, M.; Fendt, S.; Spliethoff, H. Oxygen-blown entrained flow gasification of biomass: Impact of fuel parameters and oxygen stoichiometric ratio. *Energy Fuels* **2017**, *31*, 3949–3959. [CrossRef]
8. Benevenuti, C.; Amaral, P.; Ferreira, T.; Seidl, P. Impacts of Syngas Composition on Anaerobic Fermentation. *Reactions* **2021**, *2*, 391–407. [CrossRef]
9. Kumar, A.; Jones, D.; Hanna, M. Thermochemical biomass gasification: A review of the current status of the technology. *Energies* **2009**, *2*, 556–581. [CrossRef]
10. Bengelsdorf, F.R.; Straub, M.; Dürre, P. Bacterial synthesis gas (syngas) fermentation. *Environ. Technol.* **2013**, *34*, 1639–1651. [CrossRef]
11. Vees, C.A.; Neuendorf, C.S.; Pflügl, S. Towards continuous industrial bioprocessing with solventogenic and acetogenic clostridia: Challenges, progress and perspectives. *J. Ind. Microbiol. Biotechnol.* **2020**, *47*, 753–787. [CrossRef] [PubMed]
12. Phillips, J.; Huhnke, R.; Atiyeh, H. Syngas Fermentation: A Microbial Conversion Process of Gaseous Substrates to Various Products. *Fermentation* **2017**, *3*, 28. [CrossRef]
13. Pawlak-Kruczek, H.; Wnukowski, M.; Niedzwiecki, L.; Czerep, M.; Kowal, M.; Krochmalny, K.; Zgóra, J.; Ostrycharczyk, M.; Baranowski, M.; Tic, W.J.; et al. Torrefaction as a Valorization Method Used Prior to the Gasification of Sewage Sludge. *Energies* **2019**, *12*, 175. [CrossRef]
14. Daniell, J.; Köpke, M.; Simpson, S. Commercial biomass syngas fermentation. *Energies* **2012**, *5*, 5372–5417. [CrossRef]
15. Oliveira, L.; Röhrenbach, S.; Holzmüller, V.; Weuster-Botz, D. Continuous sulfide supply enhanced autotrophic production of alcohols with Clostridium ragsdalei. *Bioresour. Bioprocess.* **2022**, 9. [CrossRef]
16. Piatek, P.; Olsson, L.; Nygård, Y. Adaptation during propagation improves *Clostridium autoethanogenum* tolerance towards benzene, toluene and xylenes during gas fermentation. *Bioresour. Technol. Rep.* **2020**, *12*, 100564. [CrossRef]
17. Mock, J.; Zheng, Y.; Mueller, A.P.; Ly, S.; Tran, L.; Segovia, S.; Nagaraju, S.; Köpke, M.; Dürre, P.; Thauer, R.K. Energy conservation associated with ethanol formation from H_2 and CO_2 in. *J. Bacteriol.* **2015**, *18*, 2965–2980. [CrossRef] [PubMed]
18. Drake, H.L.; Gössner, A.S.; Daniel, S.L. Old acetogens, new light. *Ann. N. Y. Acad. Sci.* **2008**, *1125*, 100–128. [CrossRef]
19. Ragsdale, S.W. The eastern and western branches of the Wood/Ljungdahl pathway: How the east and west were won. *BioFactors* **1997**, *6*, 3–11. [CrossRef]
20. Ragsdale, S.W.; Pierce, E. Acetogenesis and the Wood-Ljungdahl pathway of CO_2 fixation. *Biochim. Biophys. Acta* **2008**, *12*, 1873–1898. [CrossRef]
21. Schuchmann, K.; Müller, V. Autotrophy at the thermodynamic limit of life: A model for energy conservation in acetogenic bacteria. *Nat. Rev. Microbiol.* **2014**, *12*, 809–821. [CrossRef]
22. Liou, J.S.-C.; Balkwill, D.L.; Drake, G.R.; Tanner, R.S. *Clostridium carboxidivorans* sp. nov., a solvent-producing clostridium isolated from an agricultural settling lagoon, and reclassification of the acetogen *Clostridium scatologenes* strain SL1 as *Clostridium drakei* sp. nov. *Int. J. Syst. Evol. Microbiol.* **2005**, *55*, 2085–2091. [CrossRef] [PubMed]
23. Koller, M. Biotechnological approaches to generate biogenic solvents and engery carrieres from renewable resources. *Eurobiotech J.* **2023**, *7*, 96–120. [CrossRef]
24. Lee, J.; Lee, J.W.; Chae, C.G.; Kwon, S.J.; Kim, Y.J.; Lee, J.-H.; Lee, H.S. Domestication of the novel alcohologenic acetogen *Clostridium* sp. AWRP: From isolation to characterization for syngas fermentation. *Biotechnol. Biofuels* **2019**, *12*, 228. [CrossRef]
25. Abrini, J.; Naveau, H.; Nyns, E.-J. *Clostridium autoethanogenum*, sp. nov., an anaerobic bacterium that produces ethanol from carbon monoxide. *Arch. Microbiol.* **1994**, *161*, 345–351. [CrossRef]
26. Humphreys, C.M.; McLean, S.; Schatschneider, S.; Millat, T.; Henstra, A.M.; Annan, F.J.; Breitkopf, R.; Pander, B.; Piatek, P.; Rowe, P.; et al. Whole genome sequence and manual annotation of *Clostridium autoethanogenum*, an industrially relevant bacterium. *BMC Genomics.* **2015**, *16*, 1085. [CrossRef] [PubMed]
27. Weuster-Botz, D. *Process Engineering Aspects for the Microbial Conversion of C1 Gases*; Springer: Berlin/Heidelberg, Germany, 2021; Volume 180, ISBN 978-3-031-06853-9.

28. Abubackar, H.N.; Veiga, M.C.; Kennes, C. Carbon monoxide fermentation to ethanol by *Clostridium autoethanogenum* in a bioreactor with no accumulation of acetic acid. *Bioresour. Technol.* **2015**, *186*, 122–127. [CrossRef]
29. Krishna, K.V.; Bharathi, N.; George Shiju, S.; Alagesan Paari, K.; Malaviya, A. An updated review on advancement in fermentative production strategies for biobutanol using *Clostridium* spp. *Environ. Sci. Pollut. Res. Int.* **2022**, *29*, 47988–48019. [CrossRef] [PubMed]
30. Mayer, A.; Schädler, T.; Trunz, S.; Stelzer, T.; Weuster-Botz, D. Carbon monoxide conversion with Clostridium aceticum. *Biotechnol. Bioeng.* **2018**, *115*, 2740–2750. [CrossRef]
31. Liew, F.; Henstra, A.M.; Köpke, M.; Winzer, K.; Simpson, S.D.; Minton, N.P. Metabolic engineering of *Clostridium autoethanogenum* for selective alcohol production. *Metab. Eng.* **2017**, *40*, 104–114. [CrossRef]
32. Liew, F.; Henstra, A.M.; Winzer, K.; Köpke, M.; Simpson, S.D.; Minton, N.P. Insights into CO_2 fixation pathway of *Clostridium autoethanogenum* by targeted mutagenesis. *mBio* **2016**, *7*, e00427-16. [CrossRef]
33. Nagaraju, S.; Davies, N.K.; Walker, D.J.F.; Köpke, M.; Simpson, S.D. Genome editing of *Clostridium autoethanogenum* using CRISPR/Cas9. *Biotechnol. Biofuels* **2016**, *9*, 219. [CrossRef]
34. Piatek, P.; Humphreys, C.; Raut, M.P.; Wright, P.C.; Simpson, S.; Köpke, M.; Minton, N.P.; Winzer, K. Agr Quorum Sensing influences the Wood-Ljungdahl pathway in *Clostridium autoethanogenum*. *Sci. Rep.* **2022**, *12*, 411. [CrossRef]
35. Sun, X.; Atiyeh, H.K.; Huhnke, R.L.; Tanner, R.S. Syngas fermentation process development for production of biofuels and chemicals: A review. *Bioresour. Technol. Rep.* **2019**, *7*, 100279. [CrossRef]
36. Dykstra, J.C.; van Oort, J.; Yazdi, A.T.; Vossen, E.; Patinios, C.; van der Oost, J.; Sousa, D.Z.; Kengen, S.W.M. Metabolic engineering of *Clostridium autoethanogenum* for ethyl acetate production from CO. *Microb. Cell Fact.* **2022**, *21*, 243. [CrossRef]
37. Müller, A.; Köpke, M. Recombinant Microorganisms Comprising Stereospecific Diol Dehydratase Enzyme and Methods Related Thereto. U.S. Patent 9,284,564 B2, 15 March 2016.
38. Kennes, D.; Abubackar, H.N.; Diaz, M.; Veiga, M.C.; Kennes, C. Bioethanol production from biomass: Carbohydrate vs syngas fermentation. *J. Chem. Technol. Biotechnol.* **2016**, *91*, 304–317. [CrossRef]
39. Baleeiro, F.C.F.; Kleinsteuber, S.; Neumann, A.; Sträuber, H. Syngas-aided anaerobic fermentation for medium-chain carboxylate and alcohol production: The case for microbial communities. *Appl. Microbiol. Biotechnol.* **2019**, *103*, 8689–8709. [CrossRef] [PubMed]
40. Diender, M.; Stams, A.J.M.; Sousa, D.Z. Production of medium-chain fatty acids and higher alcohols by a synthetic co-culture grown on carbon monoxide or syngas. *Biotechnol. Biofuels* **2016**, *9*, 82. [CrossRef] [PubMed]
41. Bäumler, M.; Burgmaier, V.; Herrmann, F.; Mentges, J.; Schneider, M.; Ehrenreich, A.; Liebl, W.; Weuster-Botz, D. Continuous production of ethanol, 1-butanol and 1-hexanol from CO with a synthetic co-culture of clostridia applying a cascade of stirred-tank bioreactors. *Microorganisms* **2023**, *11*, 1003. [CrossRef] [PubMed]
42. Du, Y.; Zou, W.; Zhang, K.; Ye, G.; Yang, J. Advances and Applications of Clostridium Co-culture Systems in Biotechnology. *Front. Microbiol.* **2020**, *11*, 560223. [CrossRef] [PubMed]
43. He, Q.; Hemme, C.L.; Jiang, H.; He, Z.; Zhou, J. Mechanisms of enhanced cellulosic bioethanol fermentation by co-cultivation of *Clostridium* and *Thermoanaerobacter* spp. *Bioresour. Technol.* **2011**, *102*, 9586–9592. [CrossRef]
44. Valgepea, K.; de Souza Pinto Lemgruber, R.; Abdalla, T.; Binos, S.; Takemori, N.; Takemori, A.; Tanaka, Y.; Tappel, R.; Köpke, M.; Simpson, S.D.; et al. H_2 drives metabolic rearrangements in gas-fermenting *Clostridium autoethanogenum*. *Biotechnol. Biofuels* **2018**, *11*, 55. [CrossRef] [PubMed]
45. Heffernan, J.K.; Valgepea, K.; de Souza Pinto Lemgruber, R.; Casini, I.; Plan, M.; Tappel, R.; Simpson, S.D.; Köpke, M.; Nielsen, L.K.; Marcellin, E. Enhancing CO_2-valorization using *Clostridium autoethanogenum* for sustainable fuel and chemicals production. *Front. Bioeng. Biotechnol.* **2020**, *8*, 204. [CrossRef] [PubMed]
46. Kantzow, C.; Mayer, A.; Weuster-Botz, D. Continuous gas fermentation by *Acetobacterium woodii* in a submerged membrane reactor with full cell retention. *J. Biotechnol.* **2015**, *212*, 11–18. [CrossRef] [PubMed]
47. Riegler, P.; Bieringer, E.; Chrusciel, T.; Stärz, M.; Löwe, H.; Weuster-Botz, D. Continuous conversion of CO_2/H_2 with Clostridium aceticum in biofilm reactors. *Biores Technol.* **2019**, *291*, 121760. [CrossRef] [PubMed]
48. Gunes, B. A critical review on biofilm-based reactor systems for enhanced syngas fermentation processes. *Renew. Sustain. Energy Rev.* **2021**, *143*, 110950. [CrossRef]
49. Jones, S.W.; Fast, A.G.; Carlson, E.D.; Wiedel, C.A.; Au, J.; Antoniewicz, M.R.; Papoutsakis, E.T.; Tracy, B.P. CO_2 fixation by anaerobic non-photosynthetic mixotrophy for improved carbon conversion. *Nat. Commun.* **2016**, *7*, 12800. [CrossRef] [PubMed]
50. Emerson, D.F.; Stephanopoulos, G. Limitations in converting waste gases to fuels and chemicals. *Curr. Opin. Biotechnol.* **2019**, *59*, 39–45. [CrossRef] [PubMed]
51. Maru, B.T.; Munasinghe, P.C.; Gilary, H.; Jones, S.W.; Tracy, B.P. Fixation of CO_2 and CO on a diverse range of carbohydrates using anaerobic, non-photosynthetic mixotrophy. *FEMS Microbiol. Lett.* **2018**, *365*, fny039. [CrossRef]
52. Knesebeck, M.; Schäfer, D.; Schmitz, K.; Rüllke, M.; Benz, J.P.; Weuster-Botz, D. Enzymatic one-pot hydrolysis of extracted sugar beet press pulp after solid-state fermentation with an engineered Aspergillus niger strain. *Fermentation* **2023**, *9*, 582. [CrossRef]
53. Fehér, C. Novel approaches for biotechnological production and application of L-arabinose. *J. Carbohydr. Chem.* **2018**, *37*, 251–284. [CrossRef]
54. Herrera, A.; Téllez-Luis, S.J.; Ramírez, J.A.; Vázquez, M. Production of Xylose from Sorghum Straw Using Hydrochloric Acid. *J. Cereal Sci.* **2003**, *37*, 267–274. [CrossRef]

55. Wamelink, M.M.C.; Struys, E.A.; Jakobs, C. The biochemistry, metabolism and inherited defects of the pentose phosphate pathway: A review. *J. Inherit. Metab. Dis.* **2008**, *31*, 703–717. [CrossRef] [PubMed]
56. Xiao, H.; Gu, X.; Ning, Y.; Yang, Y.; Mitchell, W.J.; Jiang, W.; Yang, S. Confirmation and elimination of xylose metabolism bottlenecks in glucose phosphoenolpyruvate- dependent phosphotransferase system-deficient Clostridium acetbutylicum for simultaneous utilization of glucose, xylose, and arabinose. *Appl. Environ. Microbiol.* **2011**, *2011*, 7886–7895. [CrossRef] [PubMed]
57. Aristilde, L.; Lewis, I.A.; Park, J.O.; Rabinowitz, J.D. Hierarchy in pentose sugar metabolism in Clostridium acetobutylicum. *Appl. Environ. Microbiol.* **2015**, *4*, 1452–1462. [CrossRef] [PubMed]
58. Wu, C.; Cano, M.; Gao, X.; Lo, J.; Maness, P.; Xiong, W. A quantitative lens on anaerobic life: Leveraging the state-of-the-art fluxomics approach to explore clostridial metabolism. *Curr. Opin. Biotechnol.* **2020**, *64*, 47–54. [CrossRef]
59. Vees, C.A.; Herwig, C.; Pflügl, S. Mixotrophic co-utilization of glucose and carbon monoxide boosts ethanol and butanol productivity of continuous *Clostridium carboxidivorans* cultures. *Bioresour. Technol.* **2022**, *353*, 127138. [CrossRef]
60. Mann, M.; Munch, G.; Regestein, L.; Rehmann, L. Cultivation strategies of *Clostridium autoethanogenum* on xylose and carbon monoxide combination. *ACS Sustain. Chem. Eng.* **2020**, *8*, 2632–2639. [CrossRef]
61. Abubackar, H.N.; Fernández-Naveira, Á.; Veiga, M.C.; Kennes, C. Impact of cyclic pH shifts on carbon monoxide fermentation to ethanol by *Clostridium autoethanogenum*. *Fuel* **2016**, *178*, 56–62. [CrossRef]
62. Oliveira, L.; Rückel, A.; Nordgauer, L.; Schlumprecht, P.; Hutter, E.; Weuster-Botz, D. Comparison of syngas-fermentation Clostrida in stirred-tank bioreactors and the effects of varing syngas impurities. *Microorganisms* **2022**, *10*, 681. [CrossRef]
63. Jeverica, S.; El Sayed, F.; Čamernik, P.; Kocjančič, B.; Sluga, B.; Rottman, M.; Papst, L. Growth detection of Cutibacterium acnes from orthopaedic implant-associated infections in anaerobic bottles from BACTEC and BacT/ALERT blood culture systems and comparison with conventional culture media. *Anaerobe* **2020**, *61*, 102133. [CrossRef] [PubMed]
64. Rückel, A.; Oppelt, A.; Leuter, P.; Johne, P.; Fendt, S.; Weuster-Botz, D. Conversion of Syngas from Entrained Flow Gasification of Biogenic Residues with *Clostridium carboxidivorans* and *Clostridium autoethanogenum*. *Fermentation* **2022**, *8*, 465. [CrossRef]
65. Doll, K.; Rückel, A.; Kämpf, P.; Wende, M.; Weuster-Botz, D. Two stirred-tank bioreactors in series enable continuous production of alcohols from carbon monoxide with *Clostridium carboxidivorans*. *Bioprocess. Biosyst. Eng.* **2018**, *41*, 1403–1416. [CrossRef] [PubMed]
66. Köpke, M.; Gerth, M.L.; Maddock, D.J.; Müller, A.P.; Liew, F.; Simpson, S.D.; Patrick, W.M. Reconstruction of an acetogenic 2,3-butanediol pathway involving a novel NADPH-dependent primary-secondary acohol dehydrogenase. *Appl. Environ. Microbiol.* **2014**, *11*, 3394–3403. [CrossRef]
67. Duval, A.; Sarbu, A.; Dalmas, F.; Albertini, D.; Avérous, L. 2,3-Butanediol as a biobased chain extender for thermoplastic polyurethanes: Influence of stereochemistry on macromolecular architectures and properties. *Macromolecules* **2022**, *55*, 5371–5381. [CrossRef]
68. Köpke, M.; Mihalcea, C.; Liew, F.; Tizard, J.H.; Ali, M.S.; Conolly, J.J.; Al-Sinawi, B.; Simpson, S.D. 2,3-butanediol production by acetogenic bacteria, an alternative route to chemical synthesis, using industrial waste gas. *Appl. Environ. Microbiol.* **2011**, *77*, 5467–5475. [CrossRef]
69. Lee, C.-G.; Jo, C.Y.; Lee, K.B.; Mun, S. Optimization of a simulated-moving-bed process for continuous separation of racemic and meso-2,3-butanediol using an efficient optimization tool based on nonlinear standing-wave-design method. *Sep. Purif. Technol.* **2021**, *254*, 117597. [CrossRef]